

Chapter 1

Optical Elements

Optical manufacturers offer a wide variety of optical elements, covering almost all possible laboratory applications. The problem is not how to design what you want but how to choose what you need.

Abstract Great variety of optical elements for visible domain available on the market is summarized in seven structural sections: mirrors, simple lenses, plates and prisms, retroreflectors, beamsplitters, imaging lenses, and microscope objectives. The first section presents mirrors: types of reflecting surfaces, broadband and narrowband coatings, mounting options, typical mounting mistakes. Polarization rotation after several reflections may be unexpected. Basic functionality of simple lenses is described, beginning from the lens maker equation for the thick lens. Its derivation, however, is postponed until the [Chap. 12](#) where it is obtained from the matrix formalism (ABCD law). Spherical aberration for basic single lens geometries is presented graphically and its minimum for the plano-convex configuration is explained. Best practical lens mountings are summarized and consequences of birefringence are emphasized in context with magneto-optics ([Chap. 8](#)). Spectral transparency of various optical materials should be considered as the first priority for the ultra-violet domain. High power applications require some simple but important know-how in order to avoid breakdowns. In aspheric lenses, spherical aberration may be almost completely removed by optimizing conic coefficients. Ray tracing is presented in the form of a picture, while detailed mathematics and computer codes are left to [Chap. 12](#). Achromatic doublets is the better choice for wide spectrum, and the front surface must be chosen wisely to obtain the design performance. Steinheil and Hastings triplets are considered as the most popular choice for relay optics. Optical flat plates and prisms are discussed starting from the defocusing they produce, being installed in the focused rays. Simple practical formulas are given for estimating deviation of rays, passing through tilted flats. Along with an ordinary dispersive prism that is both chromatic and deflecting, some special types of combined prisms may be helpful to reduce either chromaticity or deflection. Functionality of reflecting prisms like penta, Amici, Porro, Dove, and Littrow is explained. The concept of the corner cube reflector can be easily understood geometrically, using three-dimensional vector presentation. Its imaging and polarizing peculiarities are also explained in context with interferometers ([Chap. 6](#)). The section devoted to beamsplitters summarizes performance

of the basic types: plates and cubes, including rather rare type—the energy separator. Among the imaging lenses, the C-mount TV lens is most frequently used. Design, formats, and recommended mounting techniques are carefully explained. Physical idea of the telecentric lens—a very popular element in machine vision—is presented in succinct form with minimum mathematics, and the design of multi-element commercial products is demystified. The last section provides practically indispensable but not widely published specifications for microscope objectives, like mounting thread diameters, tube lens focal distances, marking legend, etc. Finally, the so-called inspection objective is introduced—a handy tool to quickly assemble an electronic imaging system.

1.1 Mirrors

Mirror is a simplest optical element. Mirrors may be flat, concave or convex. The second two types are used for focusing or defocusing. As a focusing element, the concave mirror is inferior to a lens because aberrations cannot be minimized. Therefore, concave or convex mirrors are rarely used in laboratories. On the contrary, flat mirror (Fig. 1.1) is the most frequently used optical element.

The second-surface mirrors are more protected against scratches, but produce ghost reflections from the front surface. Another disadvantage is absorption inside the glass, which may be considerable in ultraviolet or infrared domains. Therefore, it is always better to use the first-surface mirrors. Although the substrate of such mirrors is practically always made of glass for the reason of better polishing, in applications with high thermal loads it may be a metal, for example aluminium or copper. For a glass substrate, the ratio of thickness to diameter must be around 5 in order to maintain flatness of the reflecting surface. When high thermal stability is needed, materials like Pyrex[®] or Zerodur[®] may be used. Pyrex[®] has low thermal expansion and is an excellent substrate for most applications. Zerodur[®] is a glass-ceramic material with thermal expansion being nominally zero. This extra stability

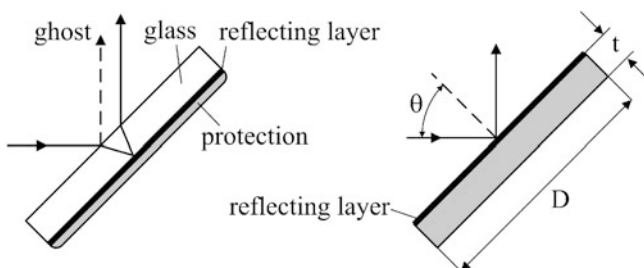


Fig. 1.1 Second-surface (at left) and first-surface (at right) mirrors

can be critical for applications, requiring diffraction limited performance. It is also worth mentioning that small-scale roughness of a typical mirror surface, measured on distances of a micrometer scale, is about 0.01 nm (standard float glass—0.02 nm), while large-scale roughness measured on a millimeter scale may vary from 0.1 to 1 nm.

Reflecting layer may be either wide-band or narrow-band. The narrow-band or monochromatic mirrors are used mostly with specific laser lines. The reflecting layer then is made as a multilayer stack of many transparent layers designed to reflect at one specific angle of incidence θ and one wavelength λ . Any change of the angle of incidence will lead to smaller reflection coefficient at this particular wavelength. Manufacturers offer mostly $\theta = 45^\circ$ narrow-band mirrors. Monochromatic mirrors are used to suppress background radiation in the systems where only one laser line is used. But their biggest advantage is that highly transparent multilayer stack introduces negligible absorption, which makes maximum reflection coefficient close to 100 %. Therefore, this type of mirrors is used when the beam path is folded many times and the delivered optical power is important. Reflection of monochromatic mirrors is based on interference, therefore, once designed for one particular wavelength such a mirror will also reflect at some other wavelengths, periodically separated from the design wavelength. How strong these ghost reflections are depends on the design, and can never be predicted. Manufacturers never disclose the entire spectral reflectance for multilayer mirrors. Therefore, in laboratory applications, the wide-band metal mirrors with aluminium or silver coatings are the better choice. In order to protect the reflecting surface from damages, a transparent rigid layer is deposited upon it. As a standard, silicon oxide (SiO) is used for protection. Typical spectral reflection for narrow-band and wide-band mirrors is shown in Fig. 1.2. Right mounting options for mirrors are shown in Fig. 1.3. Threaded O-ring should be made of plastic or soft metal like brass or aluminium in order to minimize any damage to glass. Reflecting surface must be turned to frame, otherwise O-ring would damage it during rotation. Examples of wrong mounting are shown in Fig. 1.4.

It may be assumed as a rule that metallic mirrors do not introduce any noticeable depolarization into reflected beam. However, it would be a mistake to assume the same for a system of mirrors. Consider Fig. 1.5. In the laboratory system of coordinates, inputting beam is vertically polarized, but the outgoing beam is horizontally polarized. Since people always navigate in vertical and horizontal directions, the result is also always a surprise.

1.2 Simple Lenses

A single lens is a basic optical element to focus optical beams. For high quality focusing or imaging better to use specially designed and assembled television (TV) lenses, photographic lenses, or microscope objectives, available on the market in

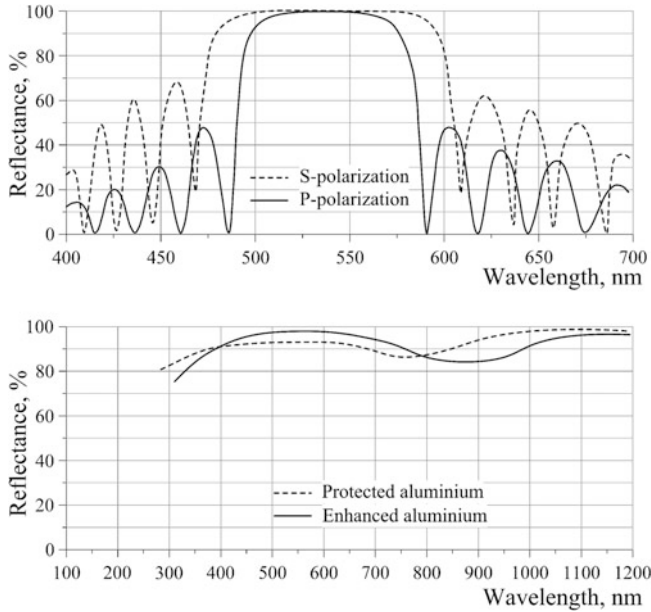


Fig. 1.2 Spectral reflectance curves: 45° narrow-band (*above*) and wide-band (*below*) mirrors

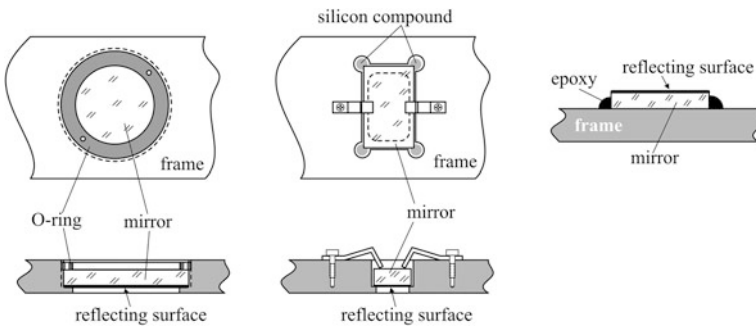


Fig. 1.3 Right mounting. Silicon compound prevents shifting

full variety. All these types of optical elements will be discussed in detail below in [Sects. 1.5–1.7](#). This section is devoted to single lenses—the simplest and cheapest focusing element. Every optical manufacturer offers numerous types of lenses, and it is important to understand what to choose for a particular application. The first thing to understand is the terminology ([Fig. 1.6](#)). The effective focal length (EFL) and principal planes P_1 , P_2 are more of a theoretical interest than of practical considerations. Usually, the design parameters are back focal length (BFL), lens diameter D , and thickness t . Sometimes, the so-called f -number is used:

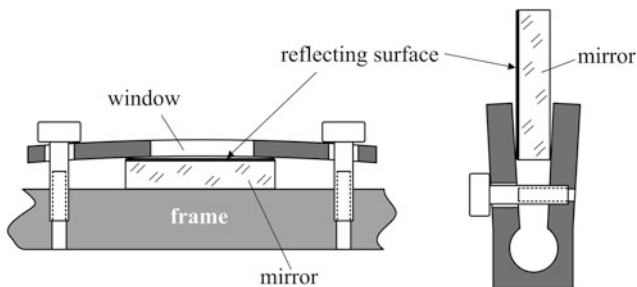
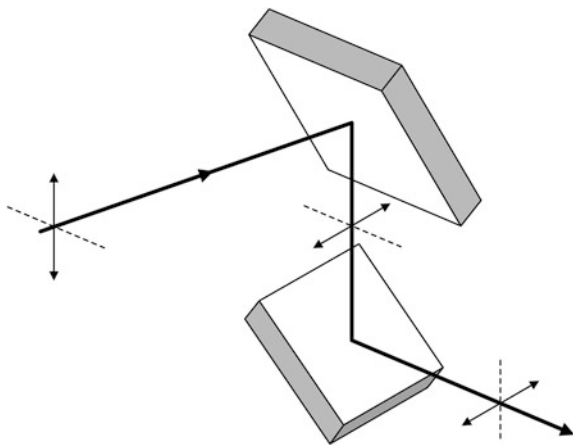


Fig. 1.4 Wrong mounting. Edges will be cleaved and reflecting surface damaged

Fig. 1.5 System of mirrors transforms polarization from vertical to horizontal



$$f - \text{number} = \frac{f}{D}.$$

The lens-maker equation determines position of the focus in air:

$$\frac{1}{f} = (n - 1) \left[\frac{1}{R_1} - \frac{1}{R_2} + \frac{t(n - 1)}{R_1 R_2 n} \right],$$

where n is the refractive index of the lens material. Obviously, various values of R_1 and R_2 make the same focal length. In order to discriminate between the lenses of different shapes but the same focal length, the Coddington shape factor q is useful:

$$q = \frac{R_2 + R_1}{R_2 - R_1}.$$

What to choose? Choose the lens with the smallest aberrations. Spherical aberration is caused by the fact that ideal spherical shape of a lens surface does not produce ideal spherical wavefront. Practically, it means that parallel laser beam will not be focused in a small point in the focus. Spherical aberration can be easily

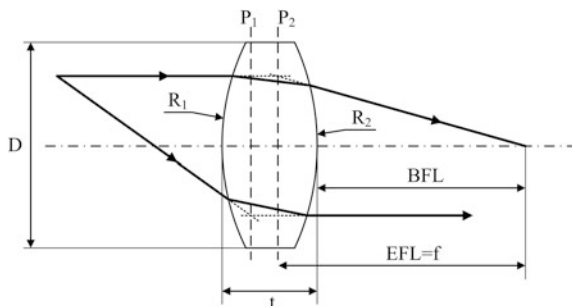


Fig. 1.6 A double convex lens. For the rays coming from left $R_1 > 0$, $R_2 < 0$

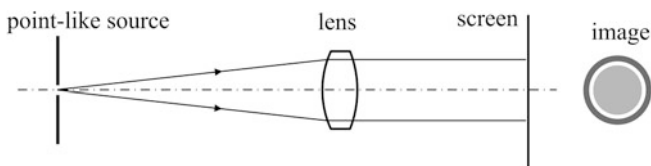


Fig. 1.7 Spherical aberration causes bright peripheral ring in a quasi-parallel beam

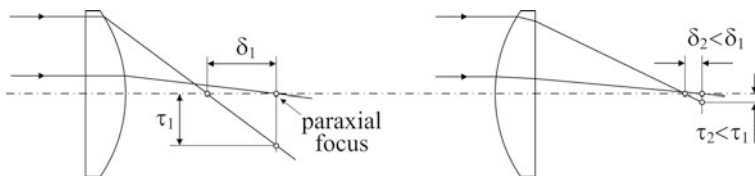


Fig. 1.8 Illumination from the flat surface causes only one refraction. Illumination from the curved surface causes two refractions, which partially compensate spherical aberration

diagnosed as shown in Fig. 1.7. Usually, this type of aberrations is dominant, and the proper choice of lens shape may minimize it. Figure 1.8 shows the difference between two plano-convex lenses of the same shape illuminated from opposite sides. The distance δ along the optical axis between the intercept of the rays that are nearly on the optical axis (paraxial rays) and the rays that go through the edge of the lens (marginal rays) is called longitudinal spherical aberration (LSA). The height τ at which these rays intercept the paraxial focal plane is called transverse spherical aberration (TSA). Figure 1.9 shows how spherical aberration varies with the shape of the lens made of BK7 glass with 100 mm focal length and f-number 10 (another notation $f/10$).

Plano-convex lens has another important practical advantage: mounting simplicity. One flat surface makes it possible to fix a lens by means of not only a standard threaded O-ring, but also gluing with ultra-violet (UV) bonder (Fig. 1.10).

UV bonder is a transparent compound that hardens when illuminated by UV radiation (UV curing). UV bonder has three important advantages over epoxy:

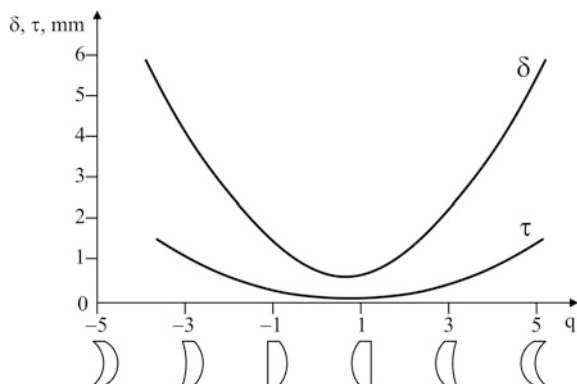


Fig. 1.9 Plano-convex shape ($q = 1$) is nearly the best. EFL is kept constant for all the shapes

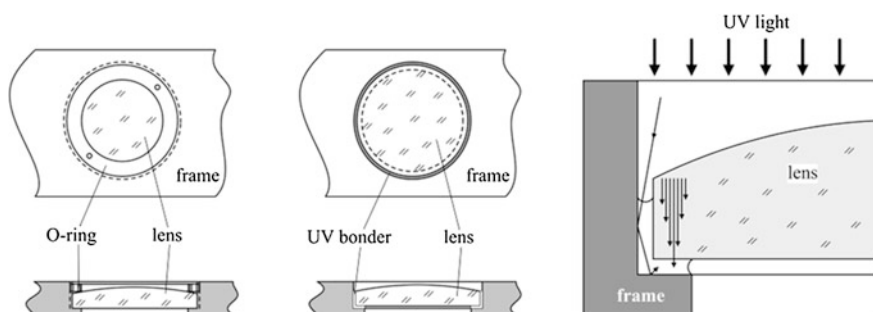


Fig. 1.10 Plano-convex lens mounting options: with threaded O-ring (*at left*), with UV bonder (*in the middle*), and mechanism of curing (*at right*). The lens housing must be deep enough to keep the lens entirely inside, preventing it from possible damage or contamination from outside

it does not hardens without UV curing, thus leaving the opportunity of disassembling the module in case when something goes awry, has low viscosity, allowing the lens to take its position under its own weight, and the ability to spread evenly over the surface due to high wetting. The technique of UV bonding requires certain skills. First, apply three-four droplets of bonder onto the rim of the lens holder (Fig. 1.11). This can be done with the help of a long whisker, like metal wire. Then wait for 10–20 min until the bonder fills the entire rim surface. After that, the lens may be put into its place, checked for its proper position, and UV cured. Standard lens materials used in visible domain, like the BK7 glass, are much less transparent in ultra-violet (UV) wing of the spectrum, below 400 nm (Fig. 1.12). However, strong UV radiation from a powerful lamp will always reach the bonder either by means of multiple reflections or through the glass bulk, as it is shown in Fig. 1.11, and harden the bonder after 1–2 min of exposure.

Manufacturers of optical tables and other mechanical equipment often suggest some standard holders for lenses, among which there are both right and wrong

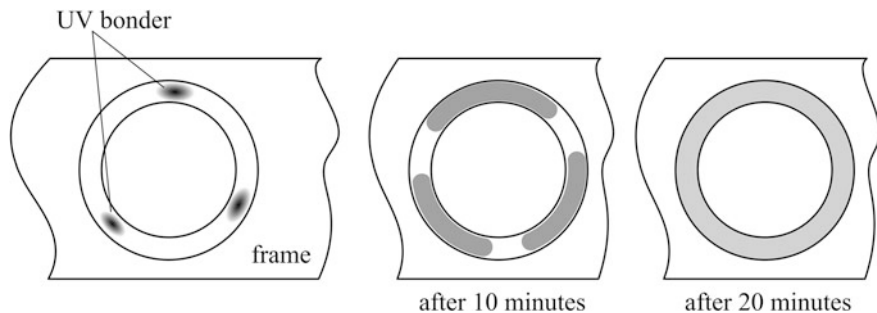


Fig. 1.11 UV bonder easily spreads over the surface

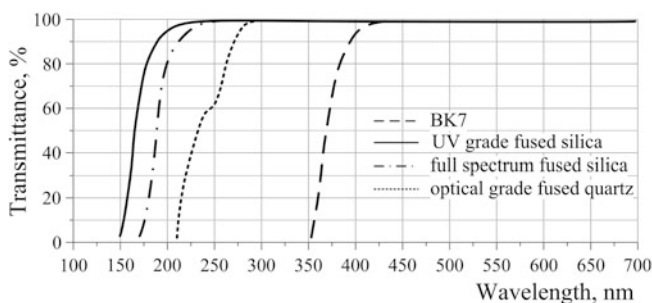


Fig. 1.12 Use UV grade fused silica lenses below 400 nm

options (Fig. 1.13). The wrong option was clearly introduced with good intentions—to hold lenses of diameters different from the standard $\frac{1}{2}$ inch. However, the result is completely unsatisfactory: a lens is always off-axis and never sits tightly in such a tripod.

For plano-concave lenses, the situation is similar (Fig. 1.14): the curved surface should be directed to the source. The only difference is that, when used with high-power lasers, reflection from the curved side may focus reflected beam back into the laser and disrupt its operation. Therefore, with high-power lasers it is recommended to place the flat surface first.

Single-element lenses with spherical surfaces still have too strong aberrations to produce fine focal spots. A possible solution is aspheric lenses, in which the shape of the surface is made to minimize aberrations for parallel input beam. If the input beam is strictly parallel, then it is possible to find exact shape of the surface, producing zero spherical aberration. For manufacturing purposes, this exact shape is usually approximated with the so-called conic formula (Fig. 1.15):

$$z(y) = \frac{y^2}{R \left(1 + \sqrt{1 - (1+k) \frac{y^2}{R^2}} \right)} + A_4 y^4 + A_6 y^6 + A_8 y^8 + \dots$$

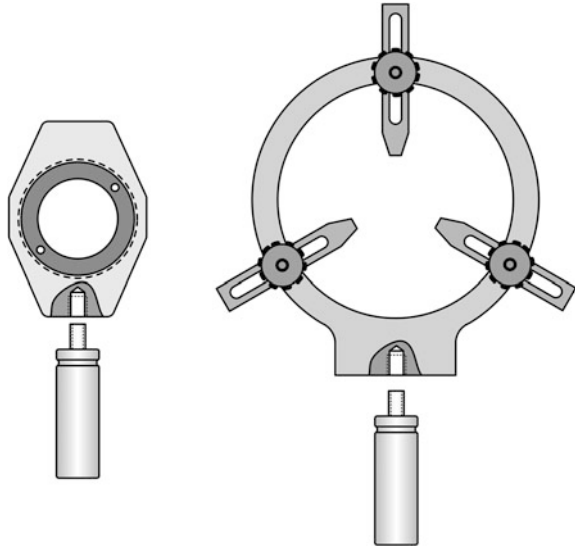


Fig. 1.13 Good (*at left*) and wrong (*at right*) accessories

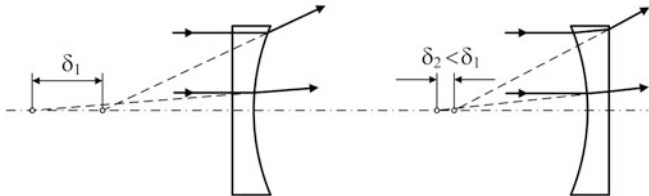
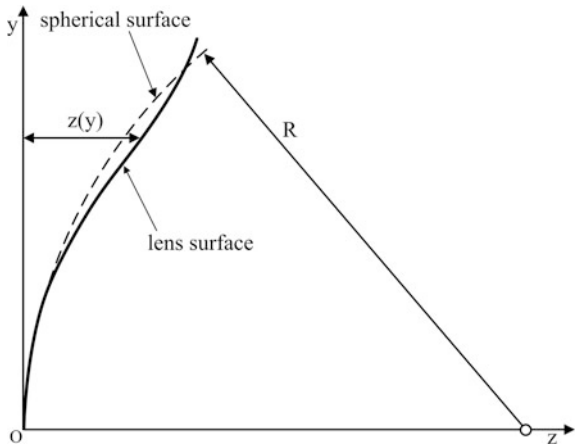


Fig. 1.14 Illumination from the flat surface causes only one refraction. Illumination from the curved surface causes two refractions, which partially compensate spherical aberration

Fig. 1.15 Optimal lens surface $z(y)$ is approximated by a conic formula



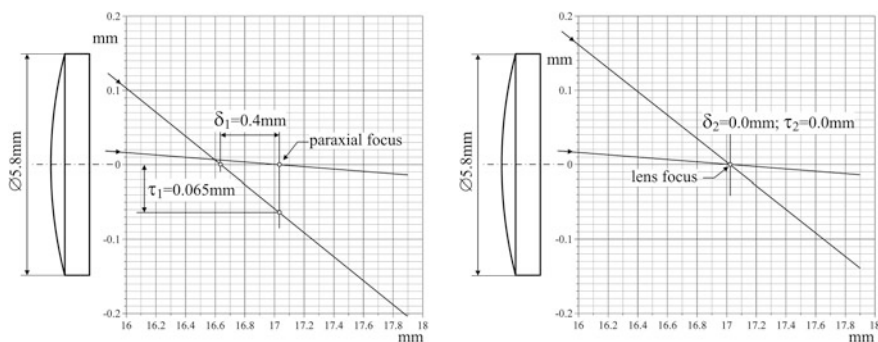
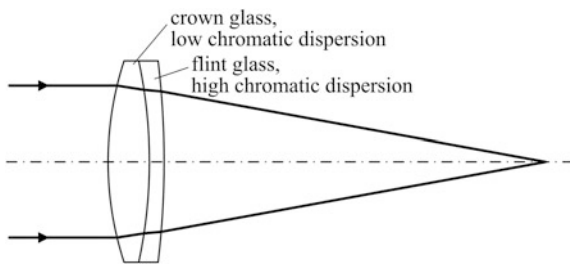


Fig. 1.16 Spherical aberrations of spherical (*at left*) and aspheric (*at right*) lenses of the same focal length and diameters

Fig. 1.17 Achromatic doublet



Parameter k is called conic coefficient, and may be either positive or negative. When $k = 0$ and all the $A_i = 0$, the formula describes spherical surface. Aspheric lenses are rather inexpensive elements because they are manufactured by molding technology. Commonly, different manufacturers offer the same product under their own names, bringing confusion to customers. However, comparing conic coefficients, it is easy to realize whether the lenses are the same or not. Another way to discover identity is to compare lens diameters, thickness, and back focal distances (BFL), which are always listed in specifications very accurately, up to the fourth digit.

The impression of how big the advantage of an aspheric lens is, comparing to its spherical analogue, can be drawn from Fig. 1.16. Paraxial foci of the two lenses practically coincide.

Whatever good the performance of an aspheric lens may be in monochromatic light, it cannot cover wide spectral range because refractive index of glass varies with wavelength, causing chromatic aberration. The common solution to this problem is the so-called achromatic doublets (Fig. 1.17)—a pair of cemented convex and concave lenses of different refractive indices. The achromatic doublet may be designed either for best chromatic compensation or for best spherical aberration performance. In the last case, manufacturer often claims diffraction-limited performance at specific wavelength, and the first surface, i.e. closest to the

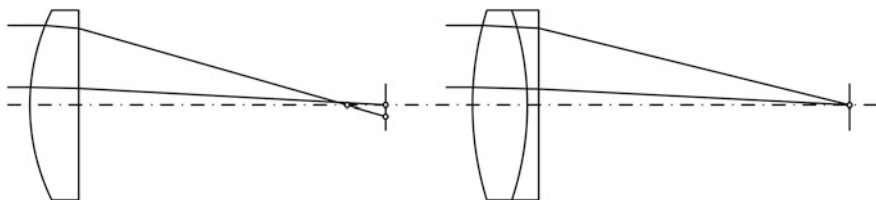
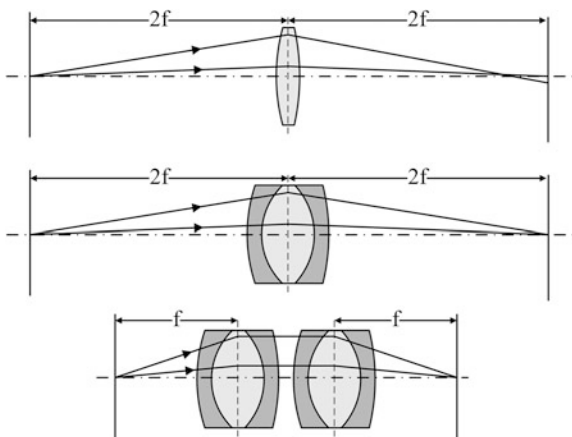


Fig. 1.18 Plano-convex lens compared with achromatic doublet

Fig. 1.19 Relay lens concept. Single lens produces noticeable spherical aberration (*above*). Corrected triplet is a better solution (*in the middle*). With two triplets the length of the system almost halves (*below*)

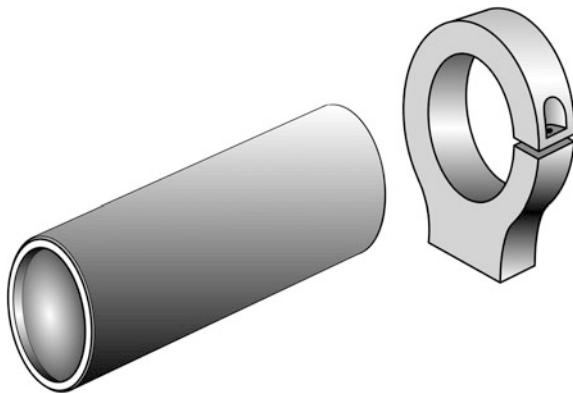


source, is always marked. If the first surface is not marked on the lens, then it is explained in detailed drawing available from the vendor or in its catalog. Lens manufacturers also offer the intermediate design, reasonably good in both chromatic and aberration compensation. Achromatic doublet has much smaller spherical aberration than the plano-convex lens (Fig. 1.18), and therefore should be the choice whenever possible.

A typical problem that may occur in optical laboratory is how to transfer an image from one plane to another. A good example is coupling galvano-scanner to front pupil of an objective. For that purpose, a variety of so-called relay lenses is available on the market. Theoretically, this can be done with only one symmetrical convex lens (Fig. 1.19). The $2f$ - $2f$ scheme not only provides unity magnification from entrance to exit but also minimal total length from image to image. Indeed, let z_1 and z_2 be the front image and exit image distances from the lens. Then lens formula

$$\frac{1}{z_1} + \frac{1}{z_2} = \frac{1}{f}$$

Fig. 1.20 Simplest mounting bracket for relay lenses



gives

$$z_1 = \frac{z_2 f}{z_2 - f}$$

and total length

$$L(z_2) = z_1 + z_2 = \frac{z_2^2}{z_2 - f}.$$

The minimum is at $z_2 = 2f$, which gives also $z_1 = 2f$.

However, spherical aberration is strong in such a system. A better solution would be to use symmetrical triplet, for example the so-called Steinheil or Hastings achromats (Fig. 1.19) with very low spherical and color aberrations. However, total length $4f$ of such a system may be too big for a particular application. The length may be roughly halved to $2f$, using the second lens (Fig. 1.19), which represents a typical scheme of a relay lens. Even more complicated optical combinations may be inside relay lenses. From practical point of view, it should be noted that manufacturers and distributors supply the product without any mounting accessories, just like a metal cylinder with optical windows at both sides. In order to install it into a system, a mounting bracket is needed (Fig. 1.20).

1.3 Plates and Prisms

A plane parallel glass plate is the most common element that can be found as optical windows of photodetectors and laser diodes, various cuvettes, beamsplitters, cover glasses, etc. There are two basic things that must be remembered: in general, a plate introduces spherical and chromatic aberration when installed in focused beam, and tilted plate displaces the beam (Fig. 1.21). For practice, it is very important to understand why a glass plate, inserted in a converging beam,

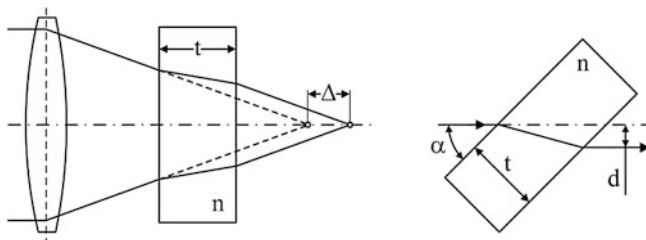
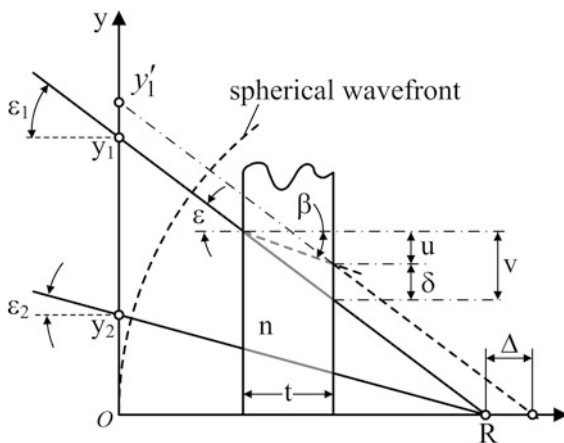


Fig. 1.21 A plate of refractive index n causes longitudinal (at left) and lateral (at right) displacements of rays

Fig. 1.22 Glass plate disrupts conical convergence



introduces aberration. Aberration means that a converging beam does not converge into one point—the focus. Consider an ideal conical beam, all rays of which come to one point located at a distance R from the vertical axis (Fig. 1.22).

If two rays converge to one focus then

$$\begin{cases} \tan \varepsilon_1 = \frac{y_1}{R} \\ \tan \varepsilon_2 = \frac{y_2}{R} \end{cases}$$

or

$$\frac{y_1}{y_2} = \frac{\tan \varepsilon_1}{\tan \varepsilon_2}.$$

When the plate is inserted, the points y_1 and y_2 shift to new locations y'_1 and y'_2 . After refraction

$$\sin \varepsilon = n \sin \beta,$$

so that

$$\delta = v - u = t \cdot (\tan \varepsilon - \tan \beta)$$

$$\begin{cases} y'_1 = y_1 + \delta_1 \\ y'_2 = y_2 + \delta_2 \end{cases}.$$

The ratio

$$\frac{y'_1}{y'_2} = \frac{R \tan \varepsilon_1 + t \left\{ \tan \varepsilon_1 - \tan \left[\arcsin \left(\frac{1}{n} \sin \varepsilon_1 \right) \right] \right\}}{R \tan \varepsilon_2 + t \left\{ \tan \varepsilon_2 - \tan \left[\arcsin \left(\frac{1}{n} \sin \varepsilon_2 \right) \right] \right\}} \neq \frac{\tan \varepsilon_1}{\tan \varepsilon_2},$$

which means that the rays does not converge to a focus. Exact focusing occurs only in two limiting cases: plate thickness $t = 0$ or refractive index $n = 1$. However, for paraxial rays, when $\sin \varepsilon \approx \varepsilon$,

$$\tan \left[\arcsin \left(\frac{1}{n} \sin \varepsilon \right) \right] \approx \frac{1}{n} \tan \varepsilon,$$

and then

$$\frac{y_1}{y_2} \approx \frac{\tan \varepsilon_1}{\tan \varepsilon_2},$$

which means that the rays approximately converge to a focus. Therefore, for paraxial focusing through thin plates, aberrations may be quit tolerable or even unnoticeable, and then the only result is axial (longitudinal) displacement of the beam:

$$\Delta = \left(1 - \frac{1}{n} \right) t.$$

Lateral displacement

$$d = t \left[1 - \sqrt{\frac{1 - \sin^2 \alpha}{n^2 - \sin^2 \alpha}} \right] \sin \alpha.$$

It is easy to remember that $d \approx t/3$ for the most common case $\alpha = 45^\circ$ and $n = 1.5$.

An ordinary prism (Fig. 1.23) can be used either for deflection or for spectral dispersion of beams. Spectral dispersion, i.e. separation of white light into components of different wavelengths (different colors), occurs due to dependence of the refractive index n on wavelength λ . In its simplest form, called the Cauchy equation, this dependence is presented as a series

$$n(\lambda) = B + \frac{C}{\lambda^2} + \frac{D}{\lambda^4} + \dots,$$

Fig. 1.23 An ordinary prism deflects and disperses light

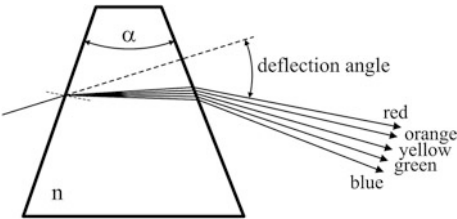


Table 1.1 Optical properties of common glass types

Material	B	C (μ^2)
Fused silica	1.4580	0.00354
Borosilicate glass BK7	1.5046	0.00420
Hard crown glass K5	1.5220	0.00459
Barium crown glass BaK4	1.5690	0.00531
Barium flint glass BaF10	1.6700	0.00743
Dense flint glass SF10	1.7280	0.01342

in which only the two first terms are important. Coefficients for common optical materials are summarized in the Table 1.1. If used as a deflector, chromatic dispersion is a negative factor, and if used as spectral selector—deflection is undesirable. For deflection of monochromatic laser beams, an ordinary prism will do well. However, for deflection of white-light beams, certain modification should be made in order to minimize spectral divergence (Fig. 1.24). In the direct-vision prism, on the contrary, angular deflection of rays is minimal.

The right-angle prisms are used for bending a beam through 90° or 180° (Fig. 1.25). In each configuration, rays undergo lossless total internal reflection that occurs when the angle of incidence becomes larger than $\arcsin(1/n)$. For $n = 1.5$ this value is 41.8° . If the entrance and exit faces are anti-reflection-coated, the total loss may be less than few percent in visible domain. The 90° rotation prism has two main disadvantages comparing to mirrors. Firstly, ghost beams reflected from the faces, even relatively weak, often produce confusing results. Secondly, when used to fold converging beams, prism acts as a glass plate, introducing aberrations. However, being used as 180° rotator, right-angle prism offers significant advantage relative to mirrors: it acts as constant-deviation reflector, redirecting incident rays exactly backwards, regardless of the prism tilt (Fig. 1.26).

In general, the constant-deviation angle is always twice the angle between two reflecting surfaces (in two-dimensional arrangements). For example, if the two reflecting surfaces make 45° then the reflected ray will always be perpendicular to the entering ray irrespective of rotations. This is the property of a penta-prism (Fig. 1.27). Unless refractive index of the penta-prism material is bigger than 2.5,

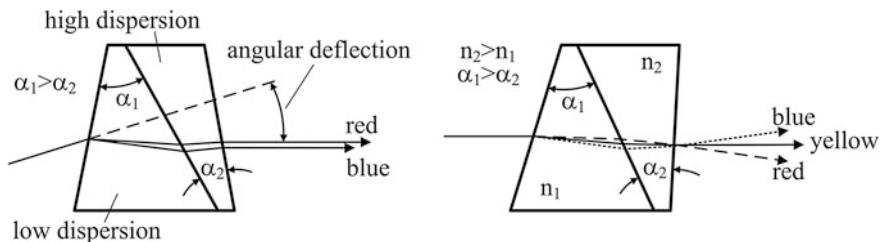


Fig. 1.24 At Left achromatic prism. The red and blue rays emerge parallel to each other, deflected from the entrance ray. At Right direct-vision dispersive prism

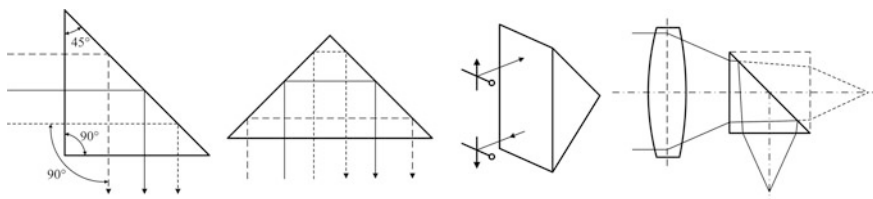
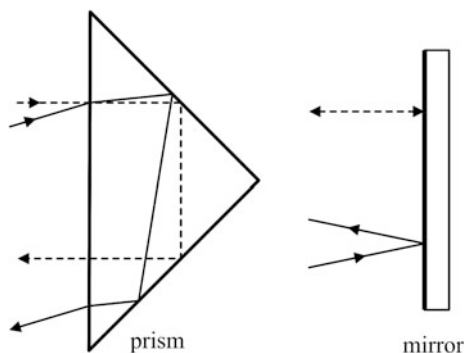


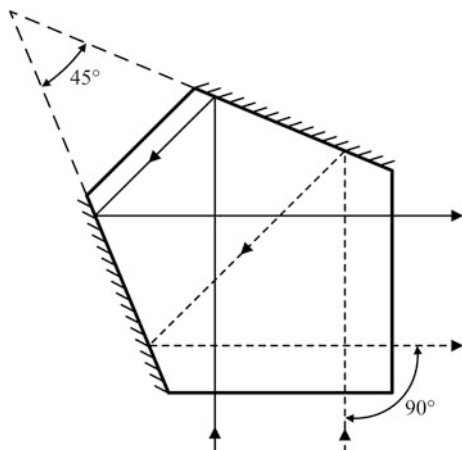
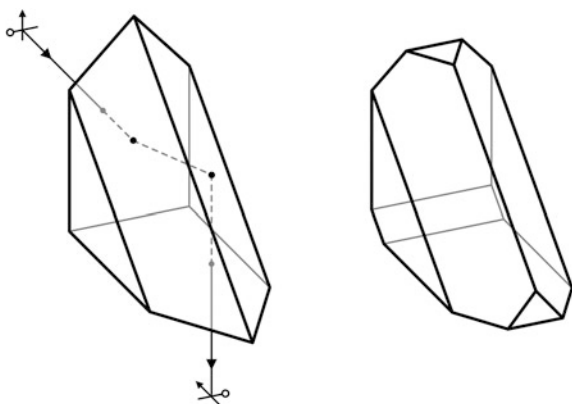
Fig. 1.25 Right-angle prism

Fig. 1.26 In the prism, the entering and exiting rays are parallel, regardless of the initial angle of incidence. Front surface refraction cancels out since the light emerges from the hypotenuse exactly at the same angle as it enters it



the total internal reflection is impossible, therefore reflecting faces are normally metallized.

Penta-prisms are often used in triangulation range-finders and also in long-travel scanners, like surface profilers, to compensate for inevitable angular rocking of a mechanical scanning stage. The image, emerging from an ordinary right-angle prism, is only half-inverted, i.e., inverted around only one axis. In order to obtain full inversion around both axes, the Amici or roof-prism may be used (Fig. 1.28). It can be obtained from an ordinary right-angle prism by replacing the hypotenuse flat face with two surfaces at 90° whose intersection lies in the hypotenuse. The ray

Fig. 1.27 Penta-prism**Fig. 1.28** Amici prism

in the figure makes approximately 60° with the roof surface instead of 45° it would be in the right-angle prism. Therefore, total internal reflection takes place for all the rays that would be reflected by an ordinary right-angle prism.

Amici prism changes the beam direction by 90° . When the beam direction must be preserved, the Porro prism may be used, which is actually a combination of two right-angle prisms (Fig. 1.29).

The Dove prism (Fig. 1.30) is an image rotating prism, and it works in total internal reflection. During recent years, this type of a prism became famous in physical laboratories owing to experiments on angular momentum of a photon. It is a common mistake to consider the Dove prism as a right-angle prism, i.e., assuming $\alpha = 45^\circ$. Although $\alpha = 45^\circ$ is a popular geometry, it is not optimal. The shortest design with minimal ratio

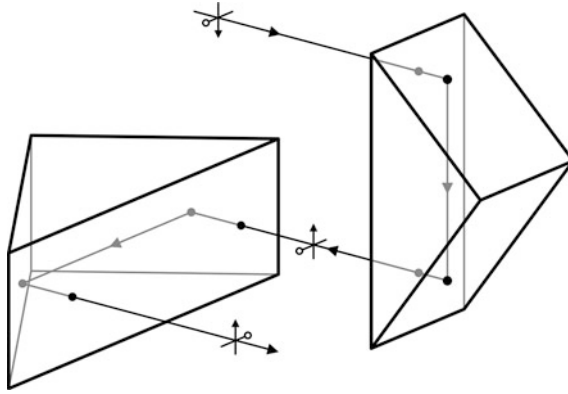


Fig. 1.29 Porro inverting prism consists of two right-angle prisms

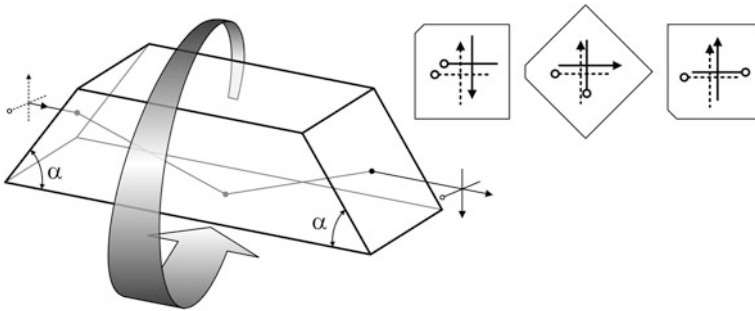


Fig. 1.30 In the Dove prism, the image is rotated twice as fast as the prism

$$\frac{\text{length}}{\text{aperture}} = \frac{1}{\sin(2\alpha)} \left[1 + \frac{\sqrt{n^2 - \cos^2 \alpha} + \sin \alpha}{\sqrt{n^2 - \cos^2 \alpha} - \sin \alpha} \right]$$

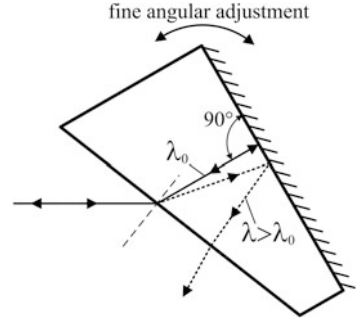
corresponds to $\alpha = 32^\circ$ for $n = 1.5$.

Among the prisms with internal reflections, the Littrow dispersion prism is frequently used for intra-cavity spectral selection in lasers (Fig. 1.31). The prism works only with metallized back face.

1.4 Retroreflectors

An optical arrangement that reflects parallel beam exactly backwards is called a retroreflector. There are two most commonly used types of retroreflectors: a corner cube reflector or a lens with a mirror in its focus. A corner cube reflector may be either a constant 180° -deviation prism that uses total internal reflection, or a

Fig. 1.31 Littrow prism.
Exact back-reflection is achieved only for one specific wavelength λ_0 , which can be changed by fine rotation of the prism



combination of three mirrors fixed together at 90° to one another (Fig. 1.32). The latter is much more expensive. Since the three-mirror assembly forms a triangular hollow, it is often called a hollow retroreflector.

The theory of a corner cube reflector is simple. In order to understand this mathematically, we have to consider reflection from a single mirror. Let \vec{k}_0 be the unity vector of the incoming beam, \vec{k}_1 —unity vector of the reflected beam, and \vec{n} —unity vector of the normal to the mirror. Then

$$\vec{k}_1 = \vec{k}_0 - 2(\vec{k}_0, \vec{n})\vec{n},$$

where (\vec{k}_0, \vec{n}) is a scalar product equal to $|\vec{k}_0| |\vec{n}| \cos(\vec{k}_0, \vec{n}) = \cos(\vec{k}_0, \vec{n})$. If there are three mirrors arranged with their normals directed along $\vec{n}_1, \vec{n}_2, \vec{n}_3$ then

$$\begin{cases} \vec{k}_1 = \vec{k}_0 - 2(\vec{k}_0, \vec{n}_1)\vec{n}_1 \\ \vec{k}_2 = \vec{k}_1 - 2(\vec{k}_1, \vec{n}_2)\vec{n}_2, \\ \vec{k}_3 = \vec{k}_2 - 2(\vec{k}_2, \vec{n}_3)\vec{n}_3 \end{cases}$$

and all the three mirrors are orthogonal. Substituting \vec{k}_1 into the formula for \vec{k}_2 , and \vec{k}_2 —into \vec{k}_3 , one gets:

$$\vec{k}_3 = \vec{k}_0 - 2(\vec{k}_0, \vec{n}_1)\vec{n}_1 - 2(\vec{k}_0, \vec{n}_2)\vec{n}_2 - 2(\vec{k}_0, \vec{n}_3)\vec{n}_3.$$

This vector is directed oppositely to \vec{k}_0 . Indeed, multiply \vec{k}_3 by \vec{k}_0 :

$$(\vec{k}_0, \vec{k}_3) = k_0^2 - 2[(\vec{k}_0, \vec{n}_1)^2 + (\vec{k}_0, \vec{n}_2)^2 + (\vec{k}_0, \vec{n}_3)^2].$$

Since $\vec{n}_1, \vec{n}_2, \vec{n}_3$ are orthogonal, the three terms in square brackets represent the sum of squared projections of the vector \vec{k}_0 onto orthogonal system of coordinate. According to Pithagoras theorem, this sum is equal to k_0^2 , and thus

$$(\vec{k}_0, \vec{k}_3) = -k_0^2 = -1,$$

which means that the angle between \vec{k}_1 and \vec{k}_3 equals to 180° .

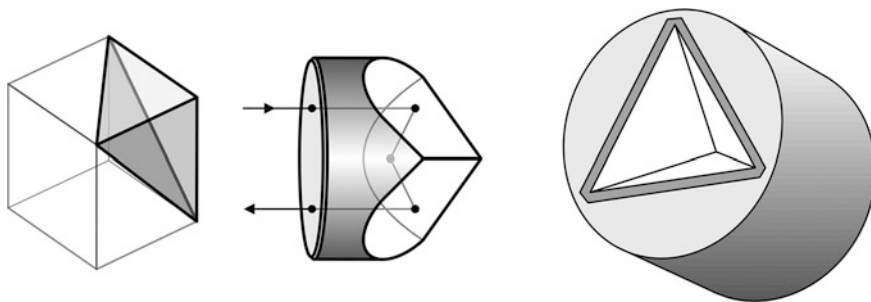


Fig. 1.32 Corner cube reflectors in the forms of a prism (*at left*) and three orthogonal mirrors (*at right*)

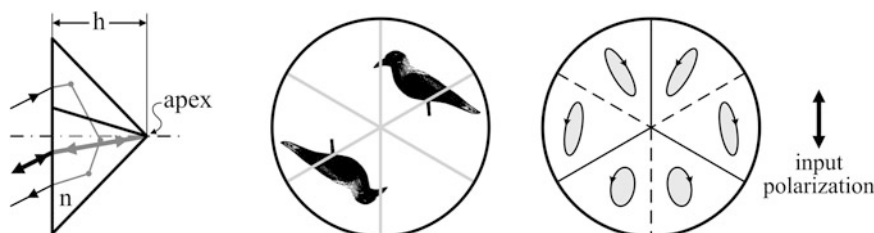
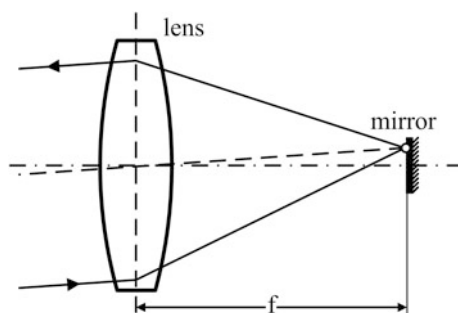


Fig. 1.33 For paraxial rays, optical path for all the rays is approximately $2hn$ (*at left*). The reflected beam is inverted over the apex. Edges do not separate the image but are visible as three symmetrical thin *dark lines*—the result of neat chamfering (*in the middle*). Prism-type retroreflectors transform input polarization in an intricate manner, generally making elliptical polarization from the linear. Each of the six visible sectors produces its own ellipticity (*at right*)

The hollow reflectors usually work better, primarily because of better angular tolerances (2 arc seconds against 20–50 of the prismatic ones). They transfer polarization of the input beam to the output without changes. Prismatic retroreflectors suffer from multiple reflections, interference fringes, and also exhibit noticeable polarization artifacts. On the other hand, they are considerably easier to clean and mount. Being illuminated by a plane wave, prismatic retroreflector also returns plane wavefront in the outgoing wave, and optical paths for all the rays are equal to that of the ray, coming to and returning from the apex (Fig. 1.33). However, polarization state of the entire cross section of the beam will not be equal to that of the illuminating wave because total internal reflection changes phases of s- and p-polarizations (p-polarization: electrical vector parallel to the plane of incidence), leading to ellipticity of the reflected beam (see Chap. 5, the Fresnel rhomb theory). This is the reason why for interferometric applications it is better to use either mirror-based or lens-based retroreflectors. Chapter 6 analyzes this topic in detail.

A lens-based retroreflector is shown in Fig. 1.34. According to geometrical optics, all the rays of a parallel beam come to a single point in the focus plane.

Fig. 1.34 In a retroreflector, the mirror is placed in the focal plane of a lens



Propagation laws are invariant to time inversion, therefore the same holds true for all the rays outgoing from this point. Therefore, a mirror placed in the focal plane of an ideal lens acts as perfect retroreflector. For a real lens with aberrations, this is true for monochromatic paraxial beams. This property of a lens-mirror combination becomes very disturbing in such applications as scanning laser microscopy, or well known compact disk writers (CD writers), because the reflected beam returns exactly to the laser and causes instability. In many cases, polarization isolation solves this problem.

1.5 Beamsplitters

The two most commonly used types of beamsplitters are the beam-splitting plates and cubes (Fig. 1.35). Almost without exception, they are designed for 45° angle of incidence and transmission ratios 50/50, 70/30, or 90/10 %. The beam-splitting cubes may be either polarizing or non-polarizing. In this section, only the non-polarizing type is considered, leaving the polarizing type for the [Chap. 5](#). Among the beam-splitting cubes, a rarer element is the so-called energy separator cube (ESC) that splits the input beam into two parallel beams. This geometry is sometimes useful in interferometry ([Chap. 6](#)).

The beam-splitting plate has only three advantages over the cube: lower price, less aberration when installed in a converging beam, and possibility to completely eliminate the ghost beam when the plate has a wedge. Aberration is smaller simply because the plate is much thinner than the cube, and the role of a wedge is explained in Fig. 1.36.

In all the other components the cube is better: better spectral uniformity of the reflection coefficient, smaller difference between transmission coefficients for s- and p-polarization, less ghosting, no displacement, easier to mount, negligible deformation under mechanical stress. In a beam-splitting plate, the beam reflects from the interface between the air and glass—two materials with very different refractive indices (1.0 and 1.5). Consequently, the reflective multilayer structure cannot be optimized equally well for the two orthogonal polarizations. In the cube,

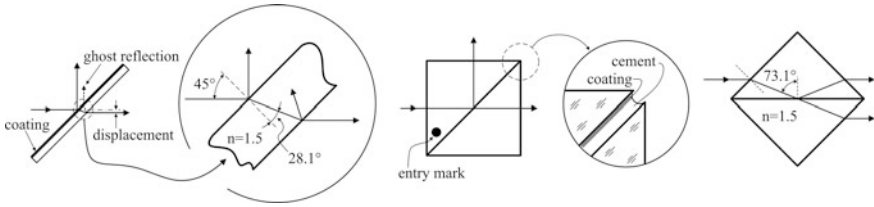


Fig. 1.35 Beam-splitting plate and cubes. The entry mark shows the face where the beam should come to. In the energy separator cube (*at right*), the multilayer coating at the diagonal interface is designed for 73.1° angle of incidence

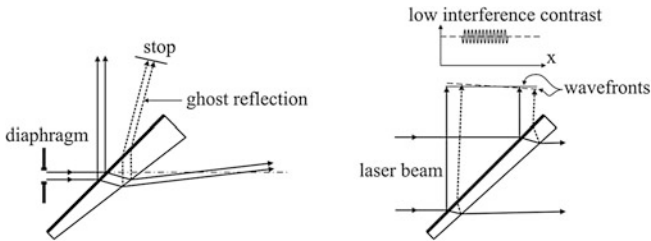


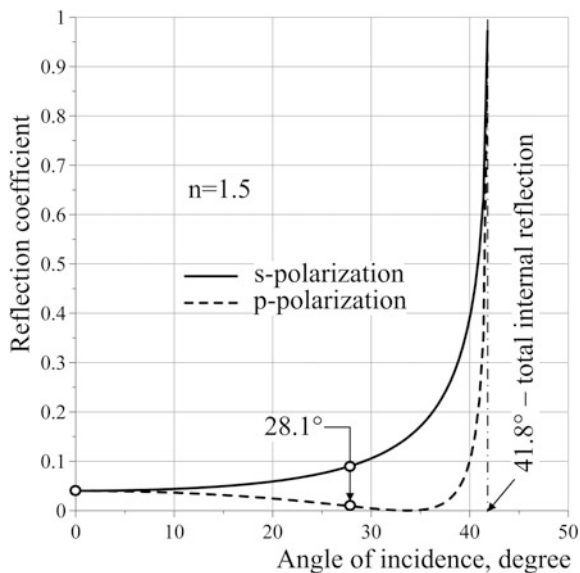
Fig. 1.36 A small wedge spatially separates the ghost beam at the expense of the deflected transmitted beam (*at left*). Much smaller wedge, about 0.5°, does not spatially separate the ghost beam, but is often used for another purpose: to destroy interference in laser beams (*at right*)

however, the reflecting interface is formed by glass and the cement—two materials with matching refractive indices, thus providing better conditions for optimization. Also, the anti-reflection coating on the second face of a 45° plate cannot decrease reflection as well as it can be done at normal incidence in the cube. It becomes clear from Fig. 1.37, showing reflection coefficients for s- and p-polarized waves at different angles of incidence in glass with refraction index $n = 1.5$. Whereas at normal incidence (zero angle) reflectivity is the same for the two polarizations (about 4 %), at 45° oriented plate (28.1° inside the glass, see Fig. 1.35) it is quite different.

Additional problem with ghost reflection is that it may create although subtle but still quite noticeable interference pattern in the form of straight fringes, especially irritating in imaging applications. This phenomenon does not happen in white light because coherence length of white light (on a micrometer scale) is much smaller than double thickness of a cube or a plate. However, with laser beams, it happens all the time, and the one way to mitigate this effect in plates is to make the plate with a tiny wedge (Fig. 1.36, right). Then the ghost wave will be tilted against the primary one by some angle θ , so that the interference between the two waves with the wavelength λ will be seen as sinusoidal modulation

$$\cos\left(\frac{2\pi}{\lambda}\theta x\right)$$

Fig. 1.37 Reflection coefficients for different polarizations of the ghost wave at the interface glass-air



with the period λ/θ . For example, with $\lambda = 0.6\mu$ and $\theta = 0.01$ rad (0.6°) the period of the interference pattern would be about 60μ , and the contrast of such a fine structure is always greatly decreased by finite divergence of the beam and spatial resolution of an optical system.

Manufacturers offer two basic types of beamsplitters: the broad-band and the laser-line ones. While the broad-band type is supposed to provide uniform reflection in the entire visible domain from 400 to 700 nm, the laser-line beamsplitters are designed for a particular laser line. Obviously, the latter ones are much simpler to design and manufacture, and as such, they have practically ideal polarization performance and transmission ratios. As to the broad-band beamsplitters, they may have very different performance, depending on the vendor. The most important factor is the equality of reflection coefficients for s- and p-polarizations. It was already explained why beam-splitting cubes provide better performance relative to beam-splitting plates. Typical curves are shown in Fig. 1.38.

Sometimes, it is preferable to have both split beams going in one direction parallel to each other. This is done by a lateral displacement beam-splitting prism (Fig. 1.39).

Although beam-splitting cubes are easy to mount on any flat surface by means of glue or epoxy, it is better to leave a chance to conveniently replace it if necessary. The first option is to establish a guiding line or plane, to which the cube can be pressed during replacement (Fig. 1.40).

Finally, it is worth mentioning that the third type of beamsplitters also exists: the so called pellicle beamsplitter—a very thin, about 5μ , polymer membrane

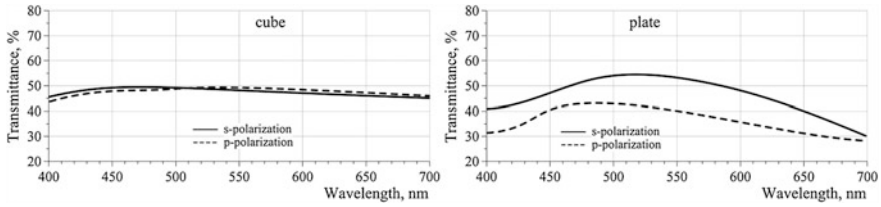


Fig. 1.38 Typical transmittance of 50/50 broad-band beam-splitting cube (*at left*) and plate (*at right*)

Fig. 1.39 Lateral displacement beamsplitter. The left 45° face acts as a total internal reflection mirror

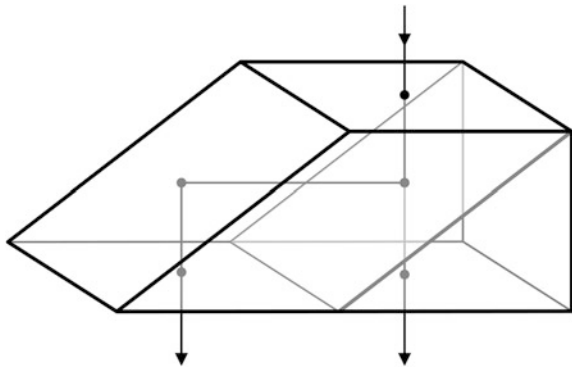
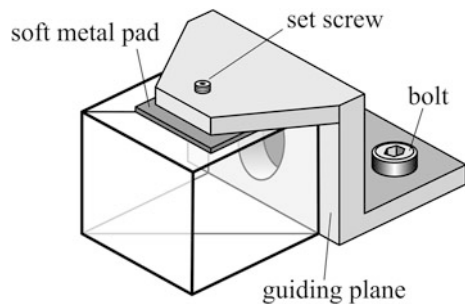
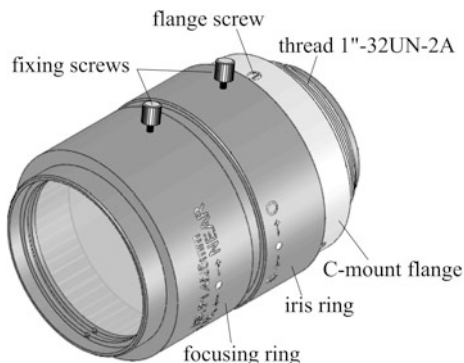


Fig. 1.40 Vertical plane of a clamping bracket accurately guides the cube to its place. Soft metal pad (aluminium, copper, or brass) protects glass from damaging



stretched over the round frame. The foil may be either coated or uncoated. The only advantage of a pellicle beamsplitter is that it practically does not introduce aberrations in focused beams, owing to its extreme thinness. This type of a beamsplitter should be avoided as much as possible: the membrane is extremely vulnerable and hygroscopic, it resonates to vibrations and acoustic noise, sensitive to airflow, produces interference fringes even in white light, and acts as a low-finesse interferometer, causing sinusoidal spectral modulation both in transmitted and reflected beams.

Fig. 1.41 Typical TV lens. The focusing and iris rings adjust image focus and optical flux. Fixing screws clamp the rings after adjustment. The C-mount flange may be removed by releasing the flange screws (usually, three screws)



1.6 Imaging Lenses

High quality white-light imaging with micrometer-scale spatial resolution over the entire field of view can only be achieved with specially designed multi-element optical systems like photographic lenses or microscopy objectives. The simplest and, therefore, cheapest representatives of this class of optical products are the television (TV) lenses, also called the CCTV lenses (charge-coupled device TV lenses). They are chromatically corrected for use with white light, designed to minimize primary aberrations like spherical and astigmatism, with manual focusing of images of distant objects in the range of 100 mm to infinity, and variable iris diaphragm. Compact, easy to mount, light-weighted, with standardized and widely accepted so-called «C-mount» flange, these lenses may be the perfect choice for many applications (Fig. 1.41). The C-mount standard includes flange-to-focus distance 17.52 mm (0.69"), the thread 1"-32TPI-2A (TPI stands for Threads Per Inch), and the threaded part length 3.8 mm (Fig. 1.42). TV lenses are available in a wide variety of fixed focal lengths, ranging from 3.5 to 75 mm. Commonly, no one is surprised that the focal length can be shorter than the flange-to-focus distance: just the ending lens is positioned closer to the image plane (Fig. 1.43, left). However, it is always a surprise that the focal length can be longer than the lens itself. The answer is that the focal length is determined as the distance from the focal point on optical axis to the intercept point with the parallel beam at the input of the lens (Fig. 1.43, right).

TV lenses are designed for various formats of charge-coupled device (CCD) matrices: 1/3", 1/2", 2/3", and even 1". CCD dimensions for these standards and corresponding image circles in the focal plane are listed in the Table 1.2, which makes it is easy to estimate diameter D of the illuminated area in the image plane, if only CCD format (Chap. 11) is known for the lens. If additionally the focal length f is known, then it is possible to determine angular field of view:

$$\omega = 2 \arctan \frac{D}{2f} \approx \frac{D}{f} \text{radian.}$$

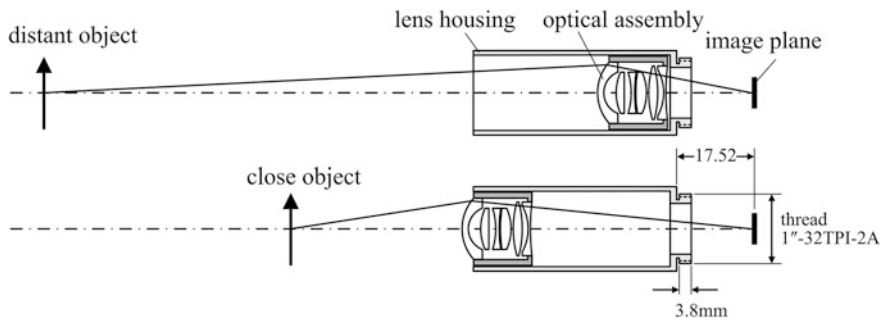


Fig. 1.42 With fixed focal length of optical assembly and constant flange-to-focus distance, the lens still can refocus to various distances due to internal shifts

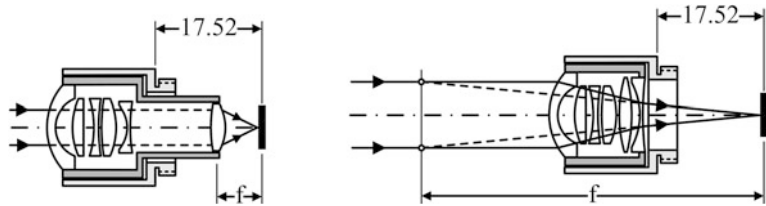


Fig. 1.43 Focal length can be either shorter (*at left*) or longer (*at right*) than the lens itself

Table 1.2 CCD formats

Type	Diagonal (mm)	Width (mm)	Height (mm)	Area (mm ²)	Image circle diameter (mm)
1"	16.0	12.8	9.6	12.3	16
1/2"	8.0	6.4	4.8	30.7	8
1/3"	6.0	4.8	3.6	17.3	6
2/3"	11.0	8.8	6.6	58.1	11
35 mm	43.3	36	24	864	43

For example, the lens is designed for 1/3" CCD format, and $f = 75$ mm. Then the field of view $\omega \approx 6/75$ radian $\approx 4^\circ$. Or $f = 12$ mm and 1/3" CCD format. Then $\omega \approx 6/12$ radian $\approx 26^\circ$.

The inner surface of the front rim of a TV lens is often threaded to adopt a filter. Unlike the C-mount thread, the filter thread cannot be standardized for all the models because input optical apertures differ significantly. However, the manufacturer always specifies filter threads for every model. It is also important to know that the C-mount flange itself can be dismantled, giving access to a dovetail flange (Fig. 1.44). In order to do that, use a fine screwdriver to release clamping screws on the C-mount flange (Fig. 1.41).

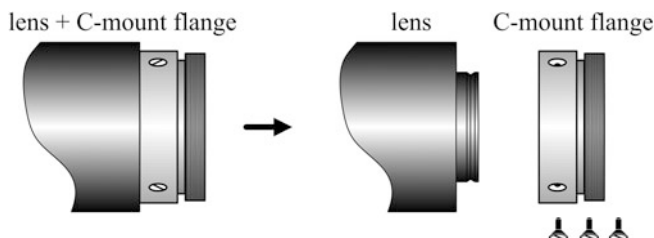


Fig. 1.44 Remove the C-mount flange to use the dovetail flange

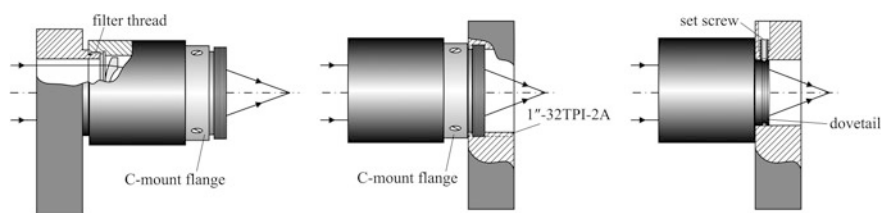


Fig. 1.45 Mounting on filter thread (*at left*), on C-mount (*in the middle*), and on dovetail (*at right*)

TV lenses are very convenient for reliable mounting. There are three options, explained in Fig. 1.45. The dovetail mounting is useful when either the thread cannot be manufactured (poorly equipped mechanical shop), or it is necessary to maintain certain orientation of a lens around its axis in order to gain access to fixing screws on focus and iris rings.

Ordinary TV lenses are not transparent in UV region below 400 nm (Fig. 1.12), and very few manufacturers offer lenses transparent down to 200 nm. But transparency alone is not enough: geometrical and chromatic aberrations must be compensated. Typically, manufacturer claims operation down to the lowest transmittable wavelength, and makes a comment that narrow band-pass optical filter is needed. This means that chromatic aberration is not compensated in the entire spectral region of glass transparency. It is normal, because the list of materials transparent in UV domain is too short to make full compensation of chromatic aberrations.

There are applications, requiring wider image circle than TV lenses can provide. For example, in spectroscopy, linear detectors 30 mm long are common. To project high-resolution images onto such big areas the camera lenses are the perfect choice (Fig. 1.46). Camera lenses were originally designed for 35 mm films (Table 1.2), therefore they can form high-quality images within wide image circle of about 40 mm in diameter. Many companies like Nikon, Canon, Zeiss manufacture camera lenses in large variety, with focal lengths ranging from 15 to 135 mm, and it is necessary to understand what to choose. Here are some guidelines. First of all, Nikon and Canon manufacture their lenses mostly for their

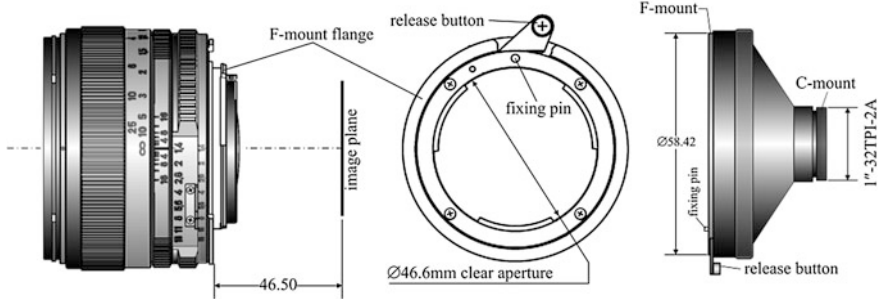


Fig. 1.46 Typical camera lens with F-mount flange (at left). F-mount to C-mount adaptor (at right)

own digital cameras, with built-in autofocus and motion-stabilization mechanisms. When disconnected from control electronics, such mechanisms are not only useless, but even dangerous, because uncontrollable motion of optical elements inside the lens changes optical scheme. Canon does not manufacture camera lenses without autofocus. Among Nikon camera lenses, it is possible to find the ones without autofocus and stabilization. According to Nikon notation, the lenses are marked as AF (autofocus), AF + S (autofocus plus stabilizer), and M (manual, i.e. no mechanics inside). So, find a lens marked «M». Zeiss, on the contrary, manufactures only lenses without autofocus and stabilization. Secondly, it is necessary to find a lens with appropriate flange. The most common type of flanges for camera lenses is the so-called F-mount, standard for Nikon and also accepted by Zeiss.

F-mount flange is rather precise piece of spring-loaded mechanics, and cannot be easily manufactured in the laboratory. For this reason, it is readily available from distributors of camera lenses or general optical equipment. Moreover, the F-to C-mount adaptors are also on the market.

A very peculiar type of a complex lens, originally developed for machine vision and providing useful properties for physical applications, is the so-called telecentric lens. Consider first the basic optical principle that determines fundamental properties of this type of a lens. Any ray, coming to an ideal lens with the focal length f parallel to its optical axis, intercepts the optical axis in the focal plane (Fig. 1.47). A paraxial parallel beam, coming to the lens at an angle α , focuses in the focal plane in a point r , making the same angle with the lens center:

$$\alpha = \arctan \frac{r}{f} \approx \frac{r}{f}.$$

If a diaphragm of radius r is placed in the focal plane, then the bundle of rays, originating at any point in front of the lens and passing through the diaphragm, form a cone with the generatrix angle α . This may be rephrased in terms of spatial frequencies filtering: since the focal plane of a lens is the Fourier-transform plane, only waves with spatial frequencies within small part $\pm r/f$ of the wave number can pass through. It is actually the basic concept of a telecentric lens.

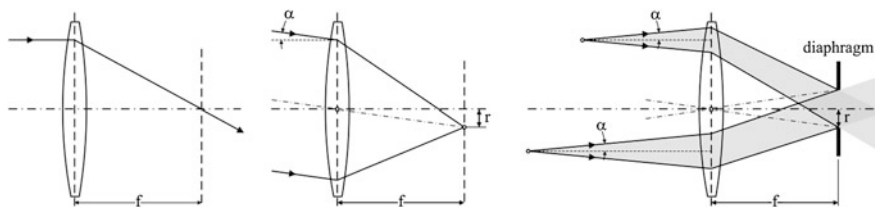


Fig. 1.47 Telecentric configuration relays only those rays that are inside a narrow fixed-angle cone around horizontal axis

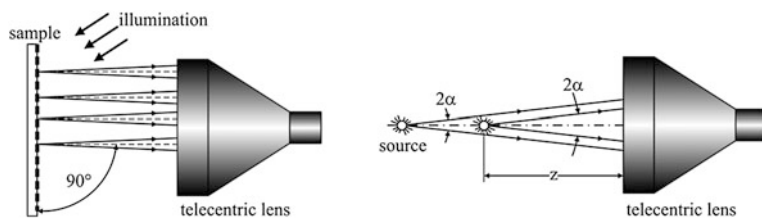


Fig. 1.48 Two basic telecentric concepts: ray cone geometry does not depend on radial position (at left) and cone angle is independent of the source axial position (at right)

For physical applications, like spectro-photometry, scatterometry, and spectral interferometry, telecentric configuration guarantees two most important concepts, which are portrayed in Fig. 1.48: the axis of the receiving cone of rays is always parallel to optical axis, and the cone angle 2α is constant independently of axial position z of the source. The second one is a very important photometric property, and should be proved with formulas.

Consider a source positioned at z in front of the lens (Fig. 1.49). We are going to analyze how the maximum angle α of rays, passing through the diaphragm, changes with z , and what is the condition for the case when α does not depend on z . Since

$$\alpha = \arctan \frac{y}{z},$$

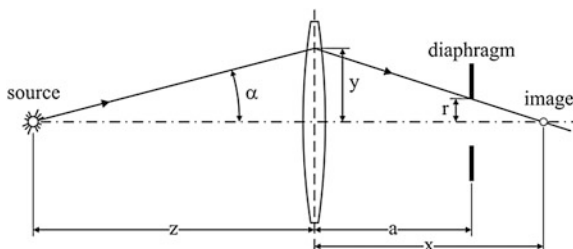
it is reasonable to analyze the ratio y/z . The image of the source is formed at x behind the lens, and the lens formula

$$\frac{1}{z} + \frac{1}{x} = \frac{1}{f}$$

gives

$$x = \frac{fz}{z - f}.$$

Fig. 1.49 The highest ray, passing through the system, is limited by a diaphragm



The highest ray that can pass through the system is determined by similarity relation:

$$\frac{r}{x-a} = \frac{y}{x}.$$

From here

$$\frac{y}{z} = \frac{rf}{fz - a(z-f)},$$

showing that, in general, y/z depends on z , except for one case $a = f$, i.e. when the diaphragm is placed in the focal plane. Then the solid angle, at which the system receives radiation from the source, is independent of the position of the source, which means constant optical flux through the system. If there is a photodetector behind the diaphragm, then its signal does not depend on the position of the source. This is the photometric property of a telecentric lens.

In order to obtain an image of the source, an imaging lens must be added to the output of the basic telecentric scheme in Fig. 1.47. Thus, conceptually, a telecentric lens may be composed of only two lenses. Real optical schemes of telecentric lenses are much more complicated, and the idea of their design should be explained to avoid confusion. First, consider how the spatial filtering concept is implemented in real design, tracing only parallel rays, coming from infinity (Fig. 1.50). Step number one: a Galilean telescope. Step number two: an short-focus objective lens, focusing the infinity image into its focal plane. Step number three: a diaphragm in this plane, which is better to call a field stop, since it is not a narrow hole any more. This is the end of spatial filtering system. Next, add the final imaging lens that forms an image of the source. The telecentric lens is ready.

There are two types of telecentric lenses basically used in practice: the object-side telecentric and the double-telecentric lenses. The difference is clear from Fig. 1.51. Telecentric lenses always end with the C-mount.

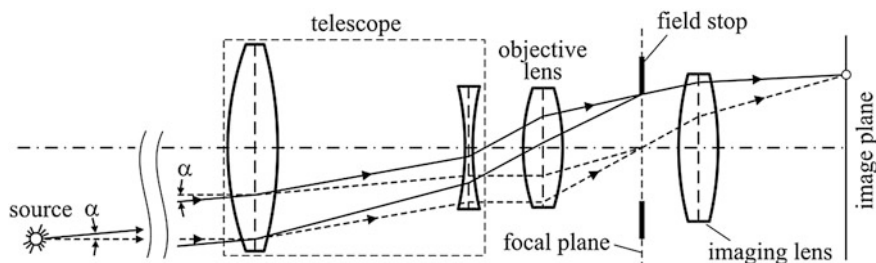
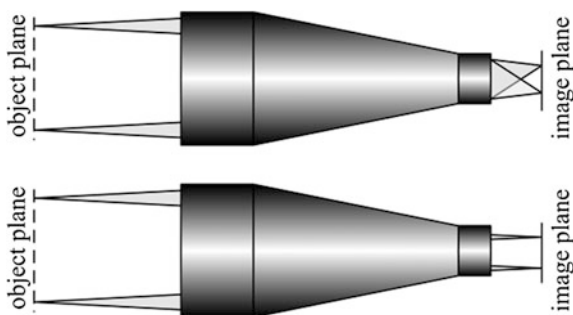


Fig. 1.50 Four steps of telecentric lens design: Galilean telescope, objective lens, field stop, and imaging lens

Fig. 1.51 The object-side (above) and double (below) telecentric lenses



1.7 Microscope Objectives

During centuries since invention of the first optical microscope, microscope objectives have become a very complicated and nearly perfect device. Originally, a microscope objective was supposed to form the image as a traditional lens, i.e. in its image plane conjugated to the object plane. This concept used to produce numerous confusions, because various manufacturers designed their objectives for different conjugation lengths. Nowadays, another concept, known as infinity conjugation, is widely used (Fig. 1.52). In it, the objective is aberration-corrected to produce parallel beam of rays at its output pupil. This means, that no image can be obtained by the objective itself until the so-called tube lens is added. This lens inherited its name from its function: to replace the long tube from the objective to the object image. It is not necessary to specify conjugation distance for every objective any more. Instead, the tube lens focal distance F determines magnification:

$$M = \frac{F}{f},$$

where f is the objective focal length. It is commonly recognized today, that infinity-corrected objectives offer more flexibility to the user in developing specific

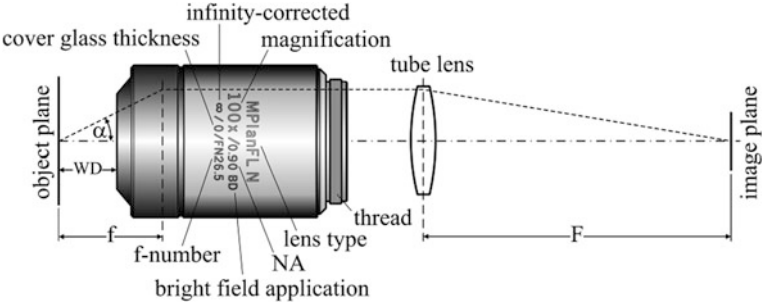


Fig. 1.52 Infinity-corrected objective requires the so-called tube lens to form an image. «WD» is the common abbreviation for working distance, «NA»—numerical aperture

Table 1.3 Specific manufacturer standards for objectives

Manufacturer	F (mm)	Thread
Zeiss	164.5	RMS standard: 0.8''-36TPI (metric 20.23 × 0.706 mm)
Nikon, Leica	200	M25 × 0.75
Olympus	180	RMS 0.8''-36TPI
Mitutoyo	200	∅26.0 mm-36TPI (metric 26 × 0.706)

applications, and the majority of the objectives on the market are of that type. Still, there are very irritating differences between manufacturers about types of the thread on their objectives and values of F used to calculate magnification M . This is explained in Table 1.3. TPI stands for Threads Per Inch, and RMS is the abbreviation for Royal Microscopy Society. Be careful: Mitutoyo defies all the standards—its thread has metric diameter but inch pitch. However, the thread length is short, therefore thread pitch may be set to metric 0.75 without any problem. Considering the aforementioned, there are two main parameters of any objective that define particular application irrelative to the manufacturer: numerical aperture (NA) and working distance (WD). Numerical aperture $NA = n \cdot \sin \alpha$ is the product of the refractive index n of the medium, interfacing with the object, and sine of the maximum ray angle α , intercepted by an objective. It is essential because, according to famous Abbe formula for an ideal lens, minimum resolving distance d depends on the wavelength λ and numerical aperture NA:

$$d = \frac{\lambda}{2 \cdot NA}.$$

Working in air, $n = 1$, therefore $NA < 1$. With immersion (oil between the objective front lens and the object), numerical aperture may reach the value 1.4.

For an ordinary objective, the working distance WD is always shorter than its focal length f (Fig. 1.53). It means that the higher the magnification is, the shorter is the working distance. For example, for $M = 100$, $WD \sim 0.3$ mm. Many applications are very sensitive to short working distance, therefore manufacturers

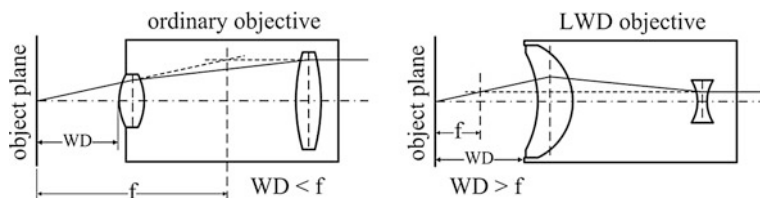


Fig. 1.53 The LWD objective always has a bigger front opening, which makes it easy to distinguish from an ordinary objective. Also, there is no concentration of rays inside the LWD objective, making it safer for laser ablation applications

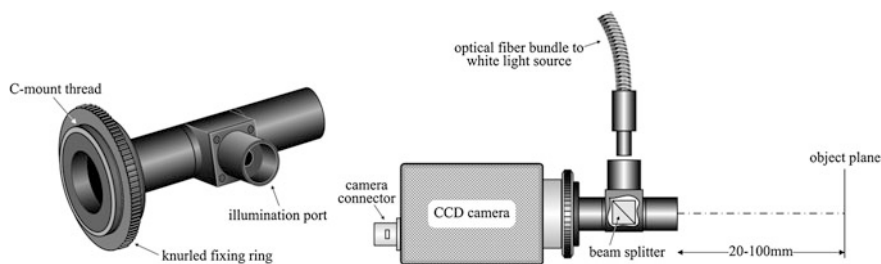


Fig. 1.54 Inspection objective is designed to be combined with a CCD camera through C-mount flange. Knurled ring on C-mount thread allows to fix illumination port at any rotation angle relative to the camera, thus choosing the best position for illumination fiber bundle

offer spring-loaded retraction stopper—a sliding front end—in some objectives with high magnification for safety reasons, in order to protect a rather expensive piece of optics from crashing into the sample during adjustment. However, industrial applications often require long working distances even with high magnification. Such objectives are called the Long Working Distance (LWD) or even Extra Long Working Distance (ELWD) objectives, and may have $WD \sim 10$ mm with $M = 100$ and $f = 2$ mm. The principle of how to do that is clearly explained in a simplified form in Fig. 1.53, and closely relates to what has been told in Fig. 1.43.

An important conclusion follows for high-power applications: do not use standard objective, because convergence of the beam inside of it may lead to damage on optical surface. Better use the LWD objectives for that purpose.

It is worth mentioning that biological applications require cover glass over a sample, and high numerical apertures of almost all the objectives would make aberrations intolerable unless the objectives were corrected for that. This feature is always marked by a special code, like in Fig. 1.52.

Industrial applications, in particular inspection technology, spawned very peculiar type of microscope objective that may be called the inspection objective (Fig. 1.54). Inspection objective is a special type of a lens designed for machine-vision applications in combination with CCD cameras (Chap. 11). Therefore, its

rear focal distance equals 17.5 mm as required by C-mount standard, and working distance is very large: from 20 to 100 mm, depending on the particular type. With the input aperture $\varnothing 12$ mm, such long working distance makes numerical aperture small, less than 0.15, and spatial resolution low, around of 5–10 μ . This, however, brings a positive feature: adjustment of the focal position is not critical. When minimum resolving distance of about 10 μ is appropriate, inspection objective is a very comfortable instrument, greatly simplifying visualization of micrometer-scale details: all that you need is the CCD camera and a white-light source.

List of Common Mistakes

- flat surface of a plano-convex lens is set first to the beam;
- focusing through glass plate or beam-splitting cube;
- folding the beam by mirrors may change polarization in the laboratory system of coordinates;
- high-power laser beam comes to a concave surface of a lens;
- an objective with internal convergence is used with high-power laser.

Further Reading

W. J. Smith, *Modern Optical Engineering*, McGraw-Hill Professional; 3rd edition (2000).
M. Born, E. Wolf, *Principles of Optics*, Pergamon Press; 4th edition (1968).
A. McLeod, *Thin Film Optical Filters*, McGraw Hill/Adam Hilger; 2nd edition (1989).
E. O'Neil, *Introduction to Statistical Optics*, Dover Publications; 4th edition (2004).

<http://www.springer.com/978-3-319-04512-2>

Practical Opto-Electronics

An Illustrated Guide for the Laboratory

Protopopov, V.

2014, IX, 393 p. 464 illus., 3 illus. in color., Hardcover

ISBN: 978-3-319-04512-2